SANDIA REPORT

SAND91—0558 • UC—814
Unlimited Release
Printed August 1992

Yucca Mountain Site Characterization Project

Automated Waste Canister Docking and Emplacement Using a Sensor-Based Intelligent Controller

W. D. Drotning

Prepared by
Sandia National Laboratories
Albuquerque, New Mexico 87185 and Livermore, California 94550
for the United States Department of Energy
under Contract DE-AC04-76DP00789

"Prepared by Yucca Mountain Site Characterization Project (YMSCP) participants as part of the Civilian Radioactive Waste Management Program (CRWM). The YMSCP is managed by the Yucca Mountain Project Office of the U.S. Department of Energy, DOE Field Office, Nevada (DOE/NV). YMSCP work is sponsored by the Office of Geologic Repositories (OGR) of the DOE Office of Civilian Radioactive Waste Management (OCRWM)."

Issued by Sandia National Laboratories, operated for the United States Department of Energy by Sandia Corporation.

Printed in the United States of America. This report has been reproduced directly from the best available copy.

Available to DOE and DOE contractors from
Office of Scientific and Technical Information
PO Box 62
Oak Ridge, TN 37831

Prices available from (615) 576-8401, FTS 626-8401

Available to the public from
National Technical Information Service
US Department of Commerce
5285 Port Royal Rd
Springfield, VA 22161

NTIS price codes
Printed copy: A03
Microfiche copy: A01

rec'd 8/31/92

SAND91-0558
Unlimited Release
Printed August, 1992

Distribution
Category UC-814

AUTOMATED WASTE CANISTER DOCKING AND EMPLACEMENT USING A SENSOR-BASED INTELLIGENT CONTROLLER

W. D. Drotning
Intelligent Systems Department II
Sandia National Laboratories
Albuquerque, NM 87185

ABSTRACT

A sensor-based intelligent control system is described that utilizes a multiple degree-of-freedom robotic system for the automated remote manipulation and precision docking of large payloads such as waste canisters. Computer vision and ultrasonic proximity sensing are used to control the automated precision docking of a large object with a passive target cavity. Real-time sensor processing and model-based analysis are used to control payload position to a precision of ± 0.5 millimeter.

102-8

This work was performed under WBS 1.2.4.2.2.

ACKNOWLEDGEMENTS

This project resulted from the efforts of several people. The design and testing of the VME-based electronics for the ultrasonic sensors was done by P. Garcia. Mechanical design of the docking system was done by S. Thunborg. J. M. Griesmeyer assisted during the early discussions of sensory systems and control concepts. The vision system was designed, implemented, and programmed by J. A. Webb. The client/server software was developed by W. M. Davidson. J. C. Fahrenholtz assisted in the robot control programming.

TABLE OF CONTENTS

LIST OF FIGURES

1.0 INTRODUCTION

Sandia National Laboratories (SNL) supports the U. S. Department of Energy's Yucca Mountain Project Site Characterization Office (YMPO) in a variety of projects, including investigations of available technologies for a potential geologic repository for the storage of nuclear waste at Yucca Mountain, Nevada. This report describes work performed at SNL for the Nuclear Waste Repository Technology (NWRT) Department 6310 by Division 1414, Intelligent Machine Systems Division. This work was performed to evaluate and demonstrate control strategies and systems for waste canister positioning, docking and emplacement during repository underground handling operations. In this investigation, a vertical docking and emplacement configuration was explicitly demonstrated, although the control principles apply to horizontal canister emplacement, as well.

Sensor-based programmable robots have potential for speeding remote manipulation operations while protecting operators from exposure to hazardous environments. Conventional master/slave manipulators have proven to be very slow in performing precision remote operations. In addition, inadvertent collisions of remotely manipulated objects with other objects in their environment increase the hazards associated with remote handling. The system described in this report utilizes non-contact and contact sensing modalities together with computing environments for the control of a robotic system for the sensor-based automated precision docking of large payloads. Docking strategies are discussed together with the results of docking experiments using model-based intelligent control.

The sensor technology and intelligent control discussed here apply to the remote manipulation of large objects in imprecisely defined environments. Specifically, these sensor and control concepts could be applied to the mating of a container of nuclear waste on a transport vehicle with an emplacement door on a vertical storage borehole at a waste repository or storage facility (Stinebaugh and Frostensen, 1986). Once the container (weighing several tons) and borehole have been mated, doors would open to allow the lowering of the waste package into the borehole. Precise docking is necessary to allow the required power connections to be made, to provide a clear vertical passage for gravity emplacement of the waste package in the

borehole, and to minimize radiation escape during the package transfer. Figure 1 shows an NWRT schematic illustration of the transporter vehicle stopped at the emplacement borehole, with the cask rotated, aligned, and docked with the borehole shielding door. Other examples which could utilize this docking technology include the remote manipulation of payloads used during cleanup of hazardous wastes, remote assembly in hazardous or inaccessible environments, and mating of large hazardous waste containers with remote processing facilities.

Because of the large masses involved, force control and use of mechanical compliance may not be feasible during docking; in fact, system criteria may require precise docking without contact between the mating objects. Remote operation is frequently desired to minimize operator exposure to hazardous environments. Multiple degrees of freedom may be required to precisely locate and mate the payload with the docking target (the borehole door). Due to the coordinated motions required with multiple degrees of freedom, manual control using teleoperation is frequently incapable of performing precision docking tasks without collision.

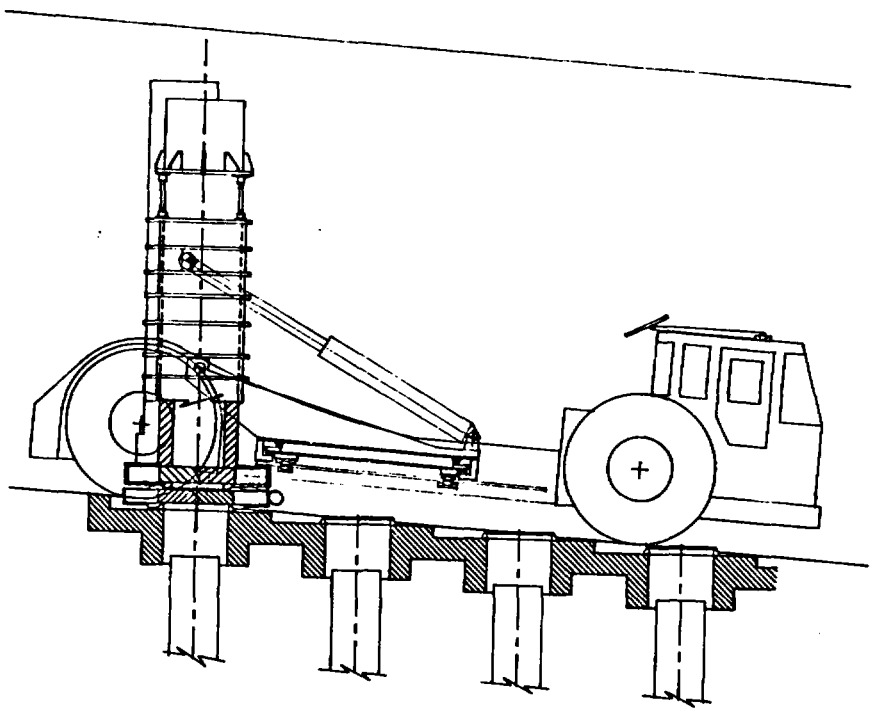

Figure 1 Transporter Vehicle at the Emplacement Borehole

Automated sensor-based docking is important, not only for safety, but to increase the speed of such operations.

A system that performs automated remote manipulation and docking requires multiple sensory systems to operate quickly and safely in imprecisely defined environments. In many applications, precision docking must be achieved at a site that is imprecisely located in both position and orientation. For example, consider the docking of the spent nuclear fuel container with the borehole door at a repository. Prior to waste insertion, radiation shield doors will be placed on the vertical storage boreholes. The emplacement of these doors will result in imprecise location and orientation, relative to fixed locations in the repository. Precise location and orientation of the entire payload transport vehicle relative to the door would add significant cost and operational time to the overall system. By employing sensors within the control system, precision control can be achieved in this imprecise environment. The use of sensory information and model-based control has been previously demonstrated in the Robotic Radiation Survey and Analysis System (RRSAS) (Thunborg, 1987), in which precision in-contact operations have been performed safely, quickly, remotely and autonomously on large imprecisely located objects. In addition, for many applications, the mating target object must remain entirely passive during the docking operations. While this constraint provides simplicity and ruggedness to the overall operation, the requirement limits the selection of available sensory technologies for use during docking.

In the system described here, computer vision and proximity sensing are used to control the precision docking of a large, heavy object to a passive target cavity. The overall strategy is to provide the sensory and control capability at each stage of docking to proceed rapidly and safely to the next stage. At the beginning, manual control by teleoperation is used to approach the target for the next stage of operation. A computer vision system takes over, automatically locating passive reference targets and controlling the motion of the system to get closer to the target goal. Next, precision ultrasonics are employed to sense the target and provide precision docking control. Finally, a combination of vision, ultrasonic, and force sensors may be used to achieve contact docking.

2.0 SYSTEM DESCRIPTION

2.1 Mechanical Configuration

The experimental apparatus shown in Figure 2 was designed to assist in the development and evaluation of sensor-based automated docking control algorithms. The test payload cylinder weighs about 70 kilograms, has a diameter of 1 meter, and contains the sensors and multiprocessor computer system to continuously monitor and control the motion of the payload during docking.

The docking bay ("door") shown in Figure 2 is the part to which the payload ("test cask") is mated during docking. The inner diameter of the door is 6 centimeters larger than the outer diameter of the payload. The door also contains a "floor" 14 centimeters from the top which supports the test payload after docking is achieved. Two side wings on the door hold targets

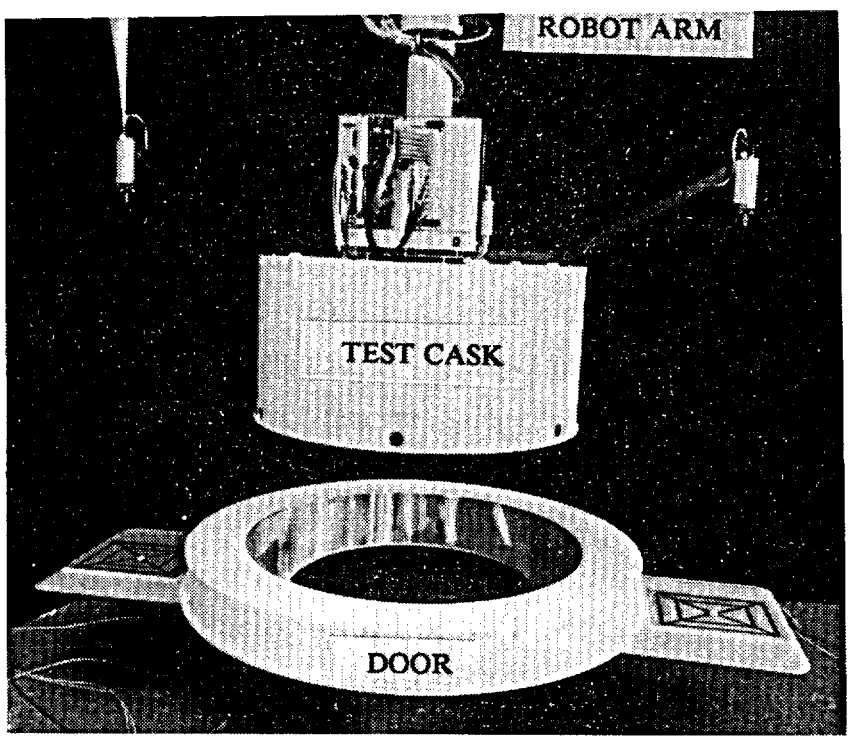

Figure 2 Docking Test Cask Payload Attached to Robot Arm Above Docking Bay Door

for the vision system; the target separation is 1.8 m. Thus, the door may be arbitrarily positioned in translation and rotation, relative to the test cask, and the intelligent docking system can still locate and successfully complete high tolerance docking maneuvers.

The test payload is positioned using the arm of a Cimcorp XR6100 gantry robot. The robot serves to simulate the function of the payload transporter system, and provides the six degrees of freedom required for docking from a random position and orientation. A force/torque sensor is attached between the robot arm and the test payload to allow force measurement and servo control during in-contact operations.

2.2 Sensor Subsystems

The block diagram in Figure 3 shows the elements of the sensor and computer systems used during docking. The dashed vertical line represents the physical separation of the items; all

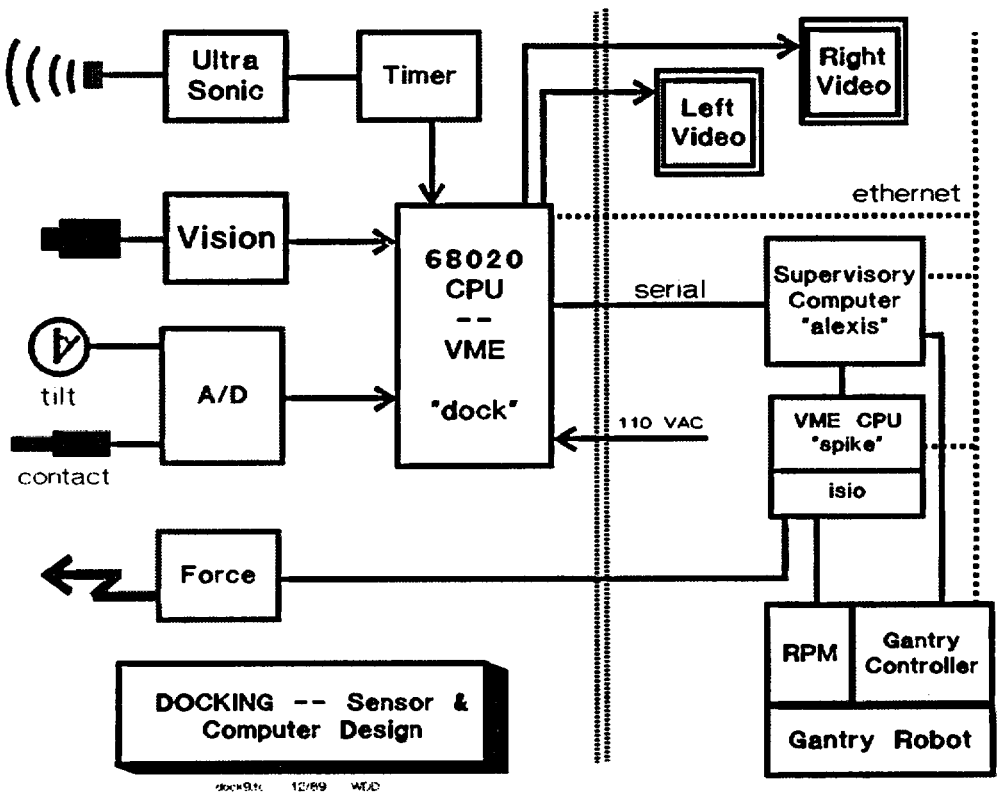

Figure 3 Block Diagram of Sensor and Computer Components for Docking System

devices left of the line are fielded on the test payload held by the robot. The devices to the right of the line are sited at the operator control station.

Multiple sensors and systems are employed for redundancy, robustness, and complementary characteristics. A schematic layout of the sensors used in the docking system is shown in Figure 4, which provides a top view schematic of the payload cask. Ultrasonics and computer vision are the two primary sensor systems used for control during automatic docking. Computer vision is used to automatically position the payload to within ± 5 millimeters in two dimensions. The ultrasonic sensors allow high precision servo-controlled docking and three-dimensional information, once the target location can be "seen" by sensors. It is important to position the payload coarsely prior to use of the ultrasonic sensors, due to their limited field of view.

The vision system on the docking test payload consists of two CCD video cameras and a

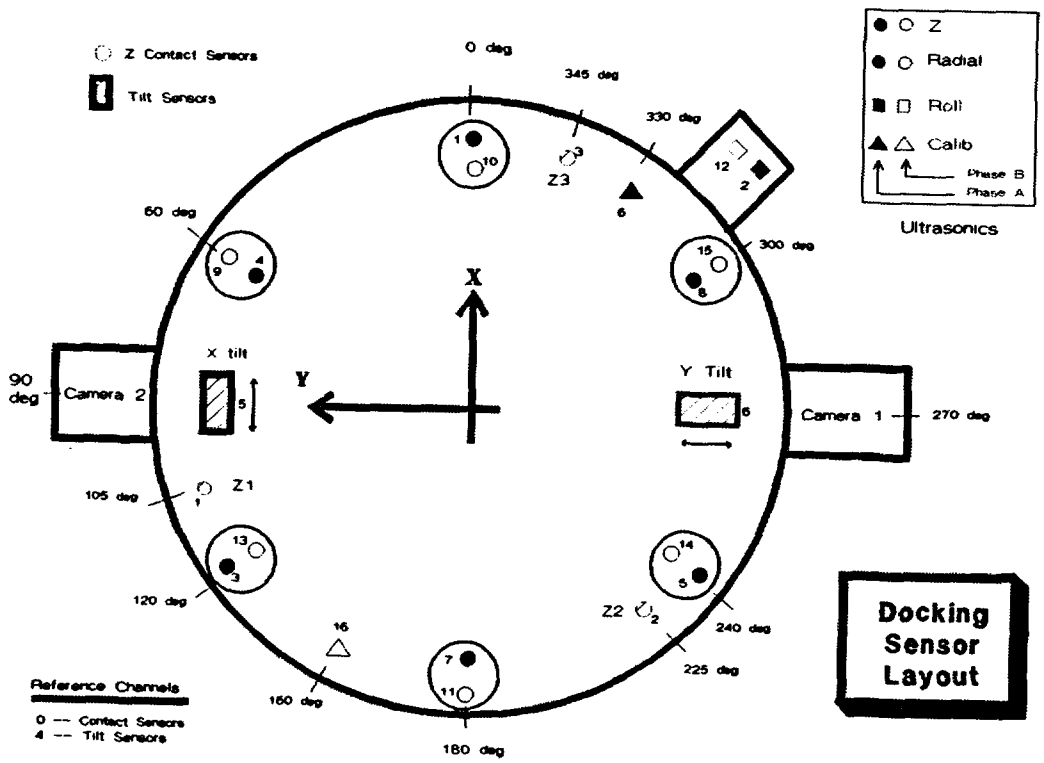

Figure 4 Top View Schematic of Sensor Layout in Test Cask Payload

VME-based digitizer and framestore system manufactured by Datacube, Inc. Simple targets (see Figure 2) on the docking bay door are automatically located by the computer vision system, providing coarse two-dimensional location information to perform the "approach" stage of docking. Remote video monitors are used to help the operator verify that the system is functioning correctly.

High frequency ultrasonics are used to acquire precision non-contact range information for docking control. Each ultrasonic sensor uses a single piezoelectric transducer, the Massa Products Corp., Model E201A/215, as both the transmitter and receiver. At the beginning of a cycle, the sensor transmits a burst of acoustic energy at 215 kilohertz, and then switches to receive mode after 0.5 milliseconds. When an echo is received, the time-of-flight yields the target range. The range resolution is on the order of 0.1 millimeter; accuracy is approximately 1 percent with calibration. The ultrasonic beam width is ± 5 degrees, which requires that target surface normals be within 5 degrees of the beam propagation direction to be detected.

A custom-designed ultrasonic control unit was developed to control and interface the ultrasonic sensors to a digital computer, all operating on a VME-bus. The analog transmit/receive driver for each sensor is based on the National Semiconductor LM1812 integrated circuit. In addition, active damping of the transmitter is used to reduce the minimum sensor range to 10 centimeters (Miller *et al.*, 1984). Maximum sensor range is approximately 60 centimeters. The system contains 16 ultrasonic sensors used for three ranging functions. Each of the two VME ultrasonic controllers is used to drive eight sensors. The controller units communicate via the P2 bus on the VME backplane. One controller serves as the master in order to synchronize the transmit cycles. The two VME ultrasonic controllers are shown in Figure 5, along with two of the ultrasonic transducers. The eight sensors driven by each board operate in phase at 100 hertz (Hz), but opposite in phase to the other board. This reduces acoustic interferences between physically adjacent sensors. In addition to the analog driver circuitry and the transmitter phasing, the control units contain digital logic to output, for each sensor, a pulse whose width represents the target range from the sensor. The eight digital pulses from each board are routed to a modified XVME-203

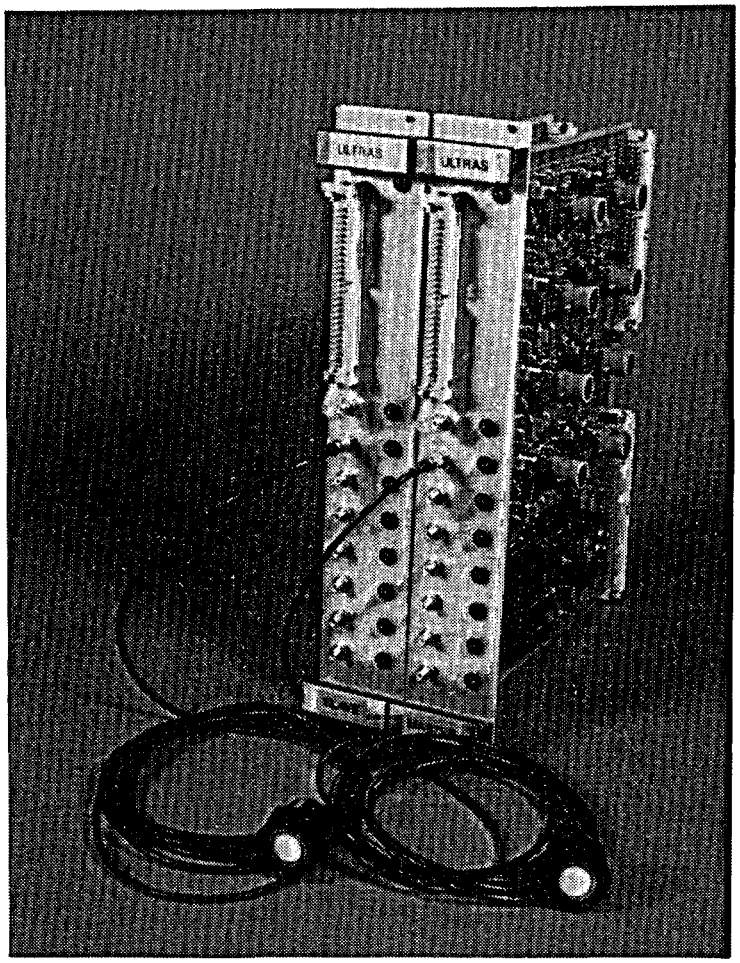

Figure 5 VME-based Ultrasonic Controllers, with Two Piezoelectric Ultrasonic Transducers

counter/timer board produced by Xycom, Inc., which uses a 4 megahertz clock to time the echo pulses to a range precision better than 0.1 millimeter. The Xycom board also generates the 100 Hz transmit/receive cycle for the master ultrasonic controller.

Six of the ultrasonic sensors are placed around the circumference of the test payload, pointing downward, to measure height from the docking bay. Six other sensors are positioned to measure range radially with respect to the center of the cylindrical test payload (see Figure 4). The down- and side-looking sensors are assembled in pairs as shown in Figure 6. The mounting configuration of the sensors uses a standoff distance from the sensor to a potential target to accommodate the minimum range of the sensor. For the radial sensors, a mirror is used to maximize the clear volume in the center of the payload. Outer apertures for the

ultrasonic sensors are about 3 centimeters diameter. Two additional ultrasonic sensors are used for real-time calibration to account for temperature, pressure and humidity effects. The current ultrasonic velocity is continuously measured and updated by timing echoes from fixed distance targets.

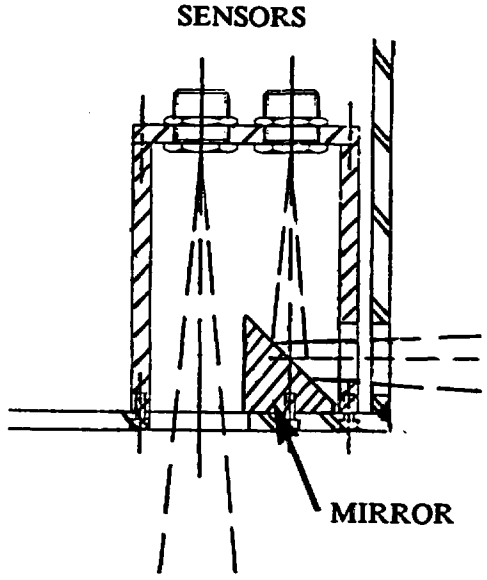

Figure 6 Down- and Side-Looking Ultrasonic Sensors

Algorithms were developed to compute range from all 16 sensors at 80 Hz. In addition, a number of derived quality measures of the data are also computed at 80 Hz, including the instantaneous target velocity relative to the sensor, whether an echo pulse is available, whether the sensor range is within specified limits, *etc*. Thus, each sensor generates range and status information for use by higher level software.

Additional sensors are used by the supervisory computing system for verification of docking and for quantitative measurement of the final docking position. Absolute tilt from vertical is measured with an inertial pendulum, and distance between the test payload and bay is measured, at close range, by contact displacement sensors attached to the payload. These sensors are used for independent verification and system performance assessment or during manual control, and not for real-time control of docking.

2.3 Computer Configuration

A self-contained VME-based computer system operating in a real-time multitasking environment was integrated into the payload (see Figure 2) to control the sensors, process the sensor data, detect sensor errors, and compute the robot motions necessary for sensor-based control of docking. The system comprises a 68020 processor (Heurikon HKV2F) with 1 megabyte of memory ("dock" in Figure 3), an ethernet controller, a combination a/d and d/a

board, three boards for the vision system, two timer boards, and two Sandia developed ultrasonic controller boards. A 12-slot VME rack with a power supply contains the VME components in a package approximately 30 by 30 by 35 centimeters, weighing less than 12 kilograms. As shown in Figure 3, ethernet is used for communication from "dock" to the robot control system. The VME-based single board computers use the VxWorks operating system produced by Wind River Systems, Inc. for real-time multitasking control. A supervisory computer is used to communicate high-level operator commands interactively to the system. The primary communication path for motion control is from "dock" to "spike", where joint position updates are sent through the serial port ("isio") to the RPM control board in the gantry robot controller every 47 milliseconds, the update rate of the robot controller. Feedback of the robot position from the robot controller returns along the same path, providing "dock" with the robot joint position coordinates necessary to compute the next robot position update from the robot kinematics and the sensor data. This communication link uses UNIX® sockets in a client/server protocol.

3.0 DOCKING CONTROL STRATEGIES AND RESULTS

Docking is divided into a hierarchical sequence of operations each with different sensor systems and control strategies. These operations are manual coarse positioning using teleoperation, automated predocking positioning in the horizontal plane using computer vision, and positioning by ultrasonic range servo control for, in order, tilt positioning about the vertical axis, displacement along the vertical axis, and precision centering in the horizontal plane. Finally, ultrasonic and force servo control are used for docking until contact with 25 kilograms force is achieved.

Initially, operator controlled teleoperation is used to coarsely position the test payload laterally over the bay to within ± 25 centimeters. Also, manual positioning using the tilt sensors may be used to align mating surfaces of the payload and bay to be parallel within ± 5 degrees, which is the requirement for ultrasonic control. An image of the horizontal positioning target visual as seen by one camera (after manual positioning) is shown in Figure 7. The target

center is the white circle (25.4 millimeters diameter) centered on the black rectangles and diagonals. The computer generated white diagonal lines show the location of the camera center. As part of a test of the automated computer vision system, a white styrofoam "peanut" has been added to the scene. Manual docking is completed when the two target circles on the door are visible in the two camera images, as in Figure 7. At this point, all six degrees of freedom (three translations and three rotations) remain to be adjusted for completion of automated docking by sensor control.

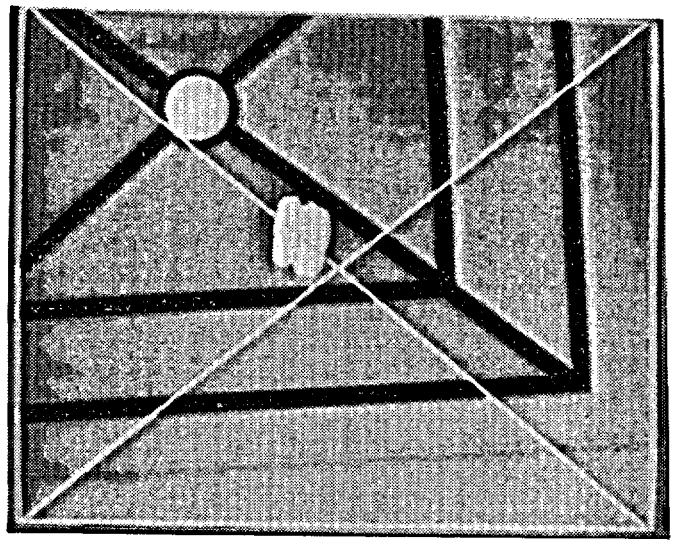

Figure 7 Image of a Target After Manual Docking Phase

The computer vision system is used next to preposition the payload in the horizontal plane in preparation for high precision docking. The contrast separation between the target and the background is the primary method used to acquire the target. However, the computer system is able to discriminate false targets, such as the styrofoam "peanut" in Figure 7, based on knowledge of the size, area, and aspect ratio (a rough measure of shape) of the target. The target image size cannot be tightly constrained, however, since the image size varies as the camera-to-target distance varies. In fact, the white peanut in Figure 7 has an area nearly identical to the true target, and a size within allowable bounds; in this case, the true target was found by shape discrimination. From the location of the targets in the two image planes, the on-board computer determines the "horizontal" plane motions (two translations and one rotation) required to center the test payload over the docking bay door, as indicated by centering the target on the camera crosshairs. The goal of this stage of docking is to align the center of the target (the white circle) with the white diagonal crosshairs. For this and subsequent motions, the directions are determined in a coordinate system attached to the payload (a robot "tool" frame), which in general is different from a coordinate frame

referenced to the docking bay. Following the automatic predocking operation, the docking targets appear as in Figure 8. Automated predocking results in the payload being positioned to within 2 millimeters in the horizontal plane, and to a rotational alignment of 0.1 degree. The size of the vision target also provides coarse range information (±3 centimeters). The large white circle outline represents a circular tolerance band around the test payload location. If the vision target falls within the band, the test payload will clear the side walls of the bay as the payload is lowered, and the operator may allow the next phase to continue safely.

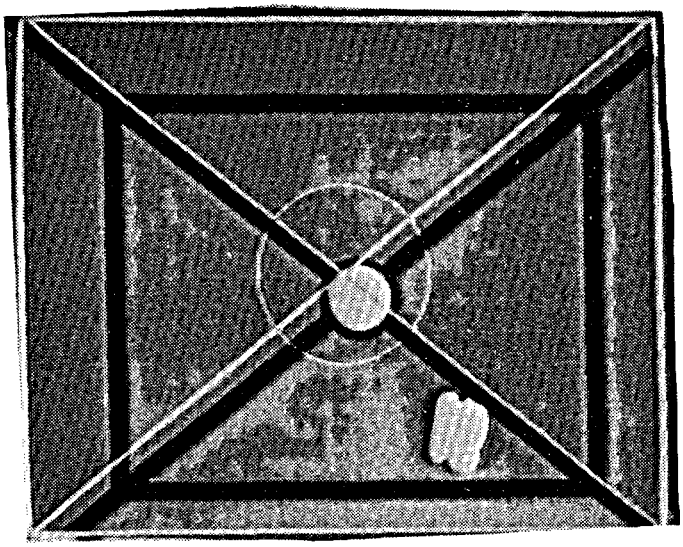

Figure 8 Image of a Target Following Computer Vision Docking Phase

Following the vision controlled predocking operation, the floor of the docking bay is within the field of view of the down-looking proximity sensors. Prior to lowering the payload to the bay under proximity servo control, the proximity sensors measure the relative orientation of the payload vertical to the door vertical. The payload's orientation is automatically adjusted to make the mating surfaces of the payload and bay parallel. This orienting operation employs data from the down-looking proximity sensors, fit in real-time by least-squares methods (see Appendix). The six down-looking sensors report target range at known (x,y) locations in the payload frame. These data are least-squares fit to a plane representing the target surface. The three parameters of the plane generate three simultaneous linear equations. The hexagonal symmetry of the sensor locations allows a direct solution, so that the parameters can be found rapidly without matrix inversion methods. The three fit parameters yield mean range to the target, and the tilt of the target plane relative to the payload, expressed as rotations about the x and y axes. From the fit parameters, the motion is computed that will tilt the test payload to align the mating surfaces to be parallel within ±0.1 degree.

Once tilt alignment has been achieved, vertical docking proceeds. In this docking operation, the test payload is lowered down into the docking bay to a preset height above the floor of the door. This is done under proximity servo control, using the ultrasonic sensor range data which is least-squares fit in real-time (<47 milliseconds) to the target plane to provide information for the motion control (see Appendix). During this procedure, the payload is lowered about 25 centimeters to a height 15 millimeters above the floor of the bay. The accuracy of the vertical position is within 0.5 millimeter.

Once the payload is lowered into the bay cavity, the side-looking proximity sensors can see the cylinder walls of the door. Range data from these sensors are used to control the final centering of the payload in the bay with high precision. The horizontal center of the cylindrical door is modeled in terms of the known door and payload radii and range from each sensor to the target wall. The data from the six sensors are least-squares fit to the model (see Appendix), and the fit parameters yield the relative two-dimensional motion vector required to center the payload in the bay. To avoid the computational complexity of solving the exact non-linear equations of a circle in real-time, the model is expressed in terms of the deviations from a circle. This provides a linear approximation, which becomes exact as the centering is completed and the payload and door centers align. Following centering by proximity control, typically to a precision of 0.3 millimeter, the camera image of a target appears as in Figure 9. The target is centered on the camera crosshairs, and the camera (white) rectangle and diagonals align with the target lines. The graph on the image is the real-time mean range data that controls the vertical docking motion. The position decrease is seen to be essentially linear from 250 millimeters above the door floor as the

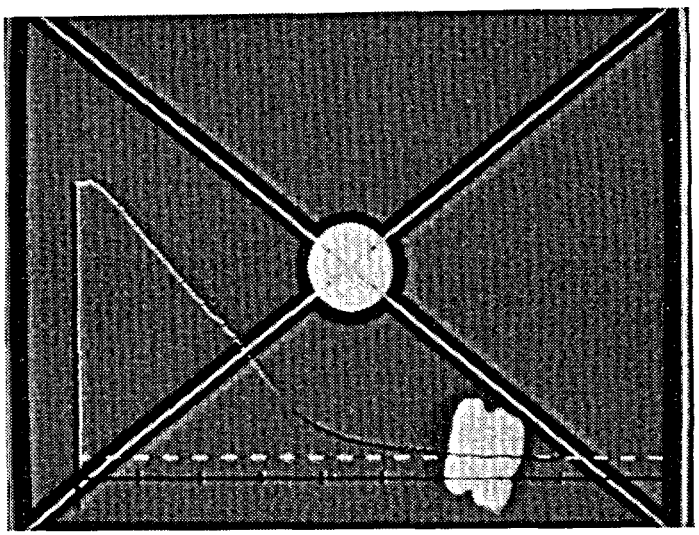

Figure 9 Image of a Target Following Ultrasonic Docking Phase

robot velocity is maintained at a maximum value of about 50 millimeters/second. As the ultrasonic sensors indicate that the payload is approaching the target resting height of 15 millimeters above the floor (the dashed horizontal line), the servo control algorithm reduces the payload velocity linearly, resulting in the observed quadratic positioning behavior.

If contact docking is desired, integration of multiple sensing modalities is employed. During contact docking, the ultrasonic proximity sensors are used to provide continuous range information to the robot controller, while the force sensor is continuously monitored. When a predetermined force change is measured in the direction of motion, the motion is stopped. All sensors are then interrogated for confirmation that the payload and door have mated. In a typical case, the payload is automatically docked to the door in about 1 minute after manual control has coarsely positioned the payload as in Figure 7.

Information from the sensor data analysis algorithms and from multiple sensors allows extensive error reporting and recovery procedures during docking. For example, during least-squares fitting of ultrasonic data to the surface types (plane or cylinder), data showing deviations that exceed predefined limits may be discarded and the analysis repeated. Data from ultrasonics and vision are used together to complement and confirm information from both types of sensors. Throughout the sequence of docking motions, information from the sensor systems provides for error detection and assurance that the next motion may be accomplished safely without collision.

4.0 CONCLUSIONS

The use of complementary sensors provides the information necessary for the remote automated manipulation and docking through six degrees of freedom of large objects with a passive bay. Vision is well-suited, first through manual control and finally by computer control, to finding and approaching a target goal. Once close approach has been achieved and the goal is nearby, precision proximity sensing is useful for real-time, non-contact position control to within fractions of a millimeter. Single-board computers may be used for real-time

sensory processing and fitting of data to models for intelligent sensor-based control of robots.

5.0 REFERENCES

Bevington, P. R., 1969, *Data Reduction and Error Analysis for the Physical Sciences*, McGraw-Hill, New York. (NNA.910523.0011)

Miller, G. L., Boie, R. A., and Sibilia, M. J., 1984, "Active Damping of Ultrasonic Transducers for Robotic Applications", Proc. 1984 IEEE Conference on Robotics and Automation, 379. (NNA.911223.0058)

Stinebaugh, R. E., and Frostenson, J. C., 1986, "Disposal of Radioactive Waste Packages in Vertical Boreholes -- A Description of the Operations and Equipment for Emplacement and Retrieval," SAND84-1010, Sandia National Laboratories, Albuquerque, NM. (NNA.891019.0276)

Thunborg, S., 1987, "A Robotic Radiation Survey and Analysis System," ANS Proc., 35th Conference on Remote Systems Technology, 133. (NNA.920130.0013)

APPENDIX A

MODEL PARAMETERS FROM LEAST-SQUARES FITS OF RANGE DATA

1.0 INTRODUCTION

The range data obtained from the ultrasonic proximity sensors are used to estimate the parameters of a model that describes the target surface. By employing multiple sensors and locations, the data set is sufficient to determine all degrees of freedom of the model. Least-squares methods (Bevington, 1969) are used to fit the data, yielding model parameter estimates and the variance of the data set from the model. This data analysis method is implemented in real-time and generates the information used for range servo control of the robot. During the docking operations, this analysis method is used for determining the parameters for two models. In the first case, range data are fit to a plane to generate tilt and vertical positioning control from the three parameters describing the plane. Secondly, range data measured radially from a cylinder are fit to a model of a parallel, non-concentric cylinder to generate the control parameters to center the two cylinders. In both cases, the assumption is made that a range measurement locates a precise target point $(x,y,z)_T$ in space, obtained from the known sensor location $(x,y,z)_s$ and the range to the target measured along the known beam propagation direction. This assumption is only approximately true, due to the finite width of the ultrasonic sensing beam. If a target is not perpendicular to the beam propagation direction, range will be reported to the nearest detected point on the target surface rather than to the point of intersection of the beam direction and the target surface. As docking proceeds and alignment improves, the target surfaces align to become perpendicular to the direction of propagation of the sensing beam, improving the accuracy of the assumption.

2.0 PLANAR TARGET

The ultrasonic proximity sensors are located in the xy-plane and transmit parallel to z in an appropriate coordinate frame. Thus, an element of the planar target detected at range z from sensor i locates a point on the target at $(x,y,z)_i$ in the coordinate frame of the sensors. The detected range from sensor i can be represented in terms of the sensor location (x,y) as

$$z_i = z(x_i,y_i). \tag{1}$$

The planar target is represented as

$$z = Ax + By + C, \tag{2}$$

where A, B, and C are the three parameters of the plane. The function G is formed from the sum of squares of the differences between the data points given by (1) and the model (2), for all points i in the data set:

$$G = \sum_i (z_i - z)^2 = \sum_i [z(x_i,y_i) - Ax_i - By_i - C]^2, \tag{3}$$

where all summations are summed over all points i. In the least-squares method, G is minimized with respect to the model parameters A, B, and C, by differentiation of Equation (3), leading to three equations in the three unknown parameters. For six sensors spaced with hexagonal symmetry on a circle of radius r, and if the coordinate frame is centered on the sensor circle, symmetry yields

$$\sum x_i = \sum y_i = \sum x_i y_i = 0. \tag{4}$$

The parameters of the plane are then found to be

$$A = (\sum x_i z_i) / 3r^2 \tag{5}$$

$$B = (\sum y_i z_i) / 3r^2 \quad \text{and} \tag{6}$$

$$C = (\sum z_i) / 6. \tag{7}$$

3.0 CYLINDRICAL TARGET

In this case, six proximity sensors provide range data radially outward from the center of a cylinder of radius R. The target surface is the inside wall of a larger diameter cylinder, parallel to but not concentric with the sensor cylinder. Since the cylinders are parallel, we can ignore the z dimension. We use a polar coordinate system (r,θ), centered on the sensor cylinder, to describe the sensor locations. The target cylinder is centered on (x_0,y_0), which represents the correction vector required to center the two cylinders. For the case of interest, the diameters of the cylinders are approximately equal, so that $x_0 << R$ and $y_0 << R$. Under this approximation, the radial deviation $d(\theta)$ can be shown to be

$$d(\theta) = x_0\cos\theta + y_0\sin\theta \tag{8}$$

where $d(\theta)$ is defined as the distance from the sensor at θ to the target, measured along a radius, minus the predicted range to a target circle of the same diameter centered on the sensor circle. By using this representation, the problem is linearized, and the complexities of the non-linear equations are avoided. Using the range measurements d_i, the function to be minimized is

$$G = \sum_i (d_i - x_0\cos\theta_i - y_0\sin\theta_i)^2. \tag{9}$$

Again, the symmetry simplifies the problem, and the solution is given by

$$x_0 = (\sum d_i\cos\theta_i)/3 \quad \text{and} \tag{10}$$

$$y_0 = (\sum d_i\sin\theta_i)/3. \tag{11}$$

Based on the residual between the model's prediction and the range data from a particular sensor, a data point in the set with a high residual may be automatically discarded, resulting in an improved parameter estimate and variance. Equations similar to (5-7) and (10-11)

obtain for four sensors in hexagonal symmetry which are used when data from a sensor is discarded. With small data sets, this iterative data analysis procedure is implemented in real-time, allowing improved immunity to a variety of noise sources in actual sensor systems, resulting in increased robustness.

APPENDIX B

Information from the Reference Information Base Used in this Report

This report contains no information from the Reference Information Base.

Candidate Information for the Reference Information Base

This report contains no candidate information for the Reference Information Base.

Candidate Information for the Site & Engineering Properties Data Base

This report contains no candidate information for the Reference Information Base.

DISTRIBUTION LIST

1 J. W. Bartlett, (RW-1)
Director
Office of Civilian Radioactive
Waste Management
U.S. Department of Energy
1000 Independence Avenue, S.W.
Washington, DC 20585

1 F. G. Peters, (RW-2)
Deputy Director
Office of Civilian Radioactive
Waste Management
U.S. Department of Energy
1000 Independence Avenue, S.W.
Washington, DC 20585

1 T. H. Isaacs (RW-4)
Office of Strategic Planning
and International Programs
OCRWM
U.S. Department of Energy
1000 Independence Avenue, S.W.
Washington, DC 20585

1 J. D. Saltzman (RW-5)
Office of External Relations
Office of Civilian Radioactive
Waste Management
U.S. Department of Energy
1000 Independence Avenue, S.W.
Washington, DC 20585

1 Samuel Rousso (RW-10)
Office of Program and Resources
Management
OCRWM
U.S. Department of Energy
1000 Independence Avenue, S.W.
Washington, DC 20585

1 J. C. Bresee (RW-10)
Office of Civilian Radioactive
Waste Management
U.S. Department of Energy
1000 Independence Avenue, S.W.
Washington, DC 20585

1 C. P. Gertz (RW-20)
Office of Geologic Disposal
Office of Civilian Radioactive
Waste Management
U.S. Department of Energy
1000 Independence Avenue, S.W.
Washington, DC 20585

1 S. J. Brocoum (RW-22)
Analysis and Verification Division
Office of Civilian Radioactive
Waste Management
U.S. Department of Energy
1000 Independence Avenue, S.W.
Washington, DC 20585

1 J. Roberts, Acting Assoc. Dir.
(RW-30)
Office of Systems and Compliance
Office of Civilian Radioactive
Waste Management
U.S. Department of Energy
1000 Independence Avenue, S.W.
Washington, DC 20585

1 J. Roberts (RW-33)
Director, Regulatory Compliance
Division
Office of Civilian Radioactive
Waste Management
U.S. Department of Energy
1000 Independence Avenue, S.W.
Washington, DC 20585

1 G. J. Parker (RW-332)
Office of Civilian Radioactive
Waste Management
U.S. Department of Energy
1000 Independence Avenue, S.W.
Washington, DC 20585

1 R. A. Milner (RW-40)
Office of Storage and Transportation
Office of Civilian Radioactive
Waste Management
U.S. Department of Energy
1000 Independence Avenue, S.W.
Washington, DC 20585

1 S. Rousso, Acting Assoc. Director
(RW-50)
Office of Contract Business
Management
Office of Civilian Radioactive
Waste Management
U.S. Department of Energy
1000 Independence Avenue, S.W.
Washington, DC 20585

1 T. Wood (RW-52)
Director, M&O Management Division
Office of Civilian Radioactive
Waste Management
U.S. Department of Energy
1000 Independence Avenue, S.W.
Washington, DC 20585

1 Dr. Garry D. Brewer
Nuclear Waste Technical Review Board
The Dana Building, Room 3516
University of Michigan
Ann Arbor, MI 48109-1115

1 Dr. Clarence R. Allen
Nuclear Waste Technical Review Board
1000 E. California Blvd.
Pasadena, CA 91106

1 Dr. John E. Cantlon, Chairman
Nuclear Waste Technical Review Board
1795 Bramble Dr.
East Lansing, MI 48823

1 Dr. Patrick A. Domenico
Nuclear Waste Technical Review Board
Geology Department
Texas A & M University
College Station, TX 77843

1 Dr. Donald Langmuir
Nuclear Waste Technical Review Board
109 So. Lookout Mountain Cr.
Golden, CO 80401

1 Dr. John J. McKetta, Jr.
Nuclear Waste Technical Review Board
Decision Focus, Inc.
4984 El Camino Real
Los Altos, CA 94062

1 Dr. D. Warner North
Nuclear Waste Technical Review Board
Decision Focus, Inc.
4984 El Camino Real
Los Altos, CA 94062

1 Dr. Dennis L. Price
Nuclear Waste Technical Review Board
1011 Evergreen Way
Blacksburg, VA 24060

1 Dr. Ellis D. Verink
Nuclear Waste Technical Review Board
4401 N.W. 18th Place
Gainesville, FL 32605

5 C. P. Gertz, Project Manager
Yucca Mountain Site Characterization
Project Office
U.S. Department of Energy
P.O. Box 98608--MS 523
Las Vegas, NV 89193-8608

1 C. L. West, Director
Office of External Affairs
DOE Field Office, Nevada
U.S. Department of Energy
P.O. Box 98518
Las Vegas, NV 89193-8518

12 Technical Information Officer
DOE Nevada Field Office
U.S. Department of Energy
P.O. Box 98518
Las Vegas, NV 89193-8518

1 P. K. Fitzsimmons, Technical
Advisor
Office of Assistant Manager for
Environmental Safety and Health
DOE Nevada Field Office
U.S. Department of Energy
P.O. Box 98518
Las Vegas, NV 89193-8518

1 D. R. Elle, Director
Environmental Protection Division
DOE Nevada Field Office
U.S. Department of Energy
P.O. Box 98518
Las Vegas, NV 89193-8518

1 Repository Licensing & Quality
Assurance
Project Directorate
Division of Waste Management
U.S. Nuclear Regulatory Commission
Washington, DC 20555

1 Senior Project Manager for Yucca
Mountain
Repository Project Branch
Division of Waste Management
U.S. Nuclear Regulatory Commission
Washington, DC 20555

1 NRC Document Control Desk
Division of Waste Management
U.S. Nuclear Regulatory Commission
Washington, DC 20555

1 P. T. Prestholt
NRC Site Representative
301 E. Stewart Ave., Room 203
Las Vegas, NV 89101

1 E. P. Binnall
Field Systems Group Leader
Building 50B/4235
Lawrence Berkeley Laboratory
Berkeley, CA 94720

1 Center for Nuclear Waste
Regulatory Analyses
6220 Culebra Road
Drawer 28510
San Antonio, TX 78284

3 W. L. Clarke
Technical Project Officer for YMP
Attn: YMP/LRC
Lawrence Livermore National
Laboratory
P.O. Box 5514
Livermore, CA 94551

1 J. A. Blink
Deputy Project Leader
Lawrence Livermore National
Laboratory
101 Convention Center Drive
Suite 280, MS 527
Las Vegas, NV 89109

4 J. A. Canepa
Technical Project Officer for YMP
N-5, Mail Stop J521
Los Alamos National Laboratory
P.O. Box 1663
Los Alamos, NM 87545

1 H. N. Kalia
Exploratory Shaft Test Manager
Los Alamos National Laboratory
Mail Stop 527
101 Convention Center Dr., Suite 820
Las Vegas, NV 89109

1 J. F. Divine
Assistant Director for
Engineering Geology
U.S. Geological Survey
106 National Center
12201 Sunrise Valley Dr.
Reston, VA 22092

1 L. R. Hayes
Technical Project Officer
Yucca Mountain Project Branch--MS 425
U.S. Geological Survey
P.O. Box 25046
Denver, CO 80225

1 V. R. Schneider
Asst. Chief Hydrologist--MS 414
Office of Program Coordination
& Technical Support
U.S. Geological Survey
12201 Sunrise Valley Drive
Reston, VA 22092

1 J. S. Stuckless
Geological Division Coordinator
MS 913
Yucca Mountain Project
U.S. Geological Survey
P.O. Box 25046
Denver, CO 80225

1 D. H. Appel, Chief
Hydrologic Investigations Program
MS 421
U.S. Geological Survey
P.O. Box 25046
Denver, CO 80225

1 E. J. Helley
Branch of Western Regional Geology
MS 427
U.S. Geological Survey
345 Middlefield Road
Menlo Park, CA 94025

1 R. W. Craig, Chief
Nevada Operations Office
U.S. Geological Survey
101 Convention Center Drive
Suite 860, MS 509
Las Vegas, NV 89109

1 D. Zesiger
U.S. Geological Survey
101 Convention Center Dr.
Suite 860, MS 509
Las Vegas, NV 89109

1 G. L. Ducret, Associate Chief
Yucca Mountain Project Division
U.S. Geological Survey
P. O. Box 25046
421 Federal Center
Denver, CO 80225

1 A. L. Flint
U.S. Geological Survey
MS 721
P.O. Box 327
Mercury, NV 89023

1 D. A. Beck
Water Resources Division
U.S. Geological Survey
6770 So. Paradise Road
Las Vegas, NV 89119

1 P. A. Glancy
U.S. Geological Survey
Federal Building, Room 224
Carson City, NV 89701

1 Sherman S. C. Wu
Branch of Astrogeology
U.S. Geological Survey
2255 N. Gemini Dr.
Flagstaff, AZ 86001

1 J. H. Sass
Branch of Tectonophysics
U.S. Geological Survey
2255 N. Gemini Dr.
Flagstaff, AZ 86001

1 DeWayne A. Campbell
Technical Project Officer for YMP
U.S. Bureau of Reclamation
Code D-3790
P.O. Box 25007
Denver, CO 80225

1 J. M. LaMonaca
Records Specialist
U.S. Geological Survey
421 Federal Center
P. O. Box 25046
Denver, CO 80225

1 W. R. Keefer
U.S. Geological Survey
913 Federal Center
P.O. Box 25046
Denver, CO 80225

1 M. D. Voegele
Technical Project Officer for YMP
Science Applications International
Corp.
101 Convention Center Dr.
Suite 407
Las Vegas, NV 89109

2 L. D. Foust
Nevada Site Manager
TRW Environmental Safety Systems
101 Convention Center Drive
Suite 540, MS 423
Las Vegas, NV 89109

1 C. E. Ezra
YMP Support Office Manager
EG&G Energy Measurements, Inc.
MS V-02
P.O. Box 1912
Las Vegas, NV 89125

1 E. L. Snow, Program Manager
Roy F. Weston, Inc.
955 L'Enfant Plaza, Southwest
Washington, DC 20024

1 Technical Information Center
Roy F. Weston, Inc.
955 L'Enfant Plaza, Southwest
Washington, DC 20024

1 D. Hedges, Vice President,
Quality Assurance
Roy F. Weston, Inc.
4425 Spring Mountain Road, Suite 300
Las Vegas, NV 89102

1 D. L. Fraser, General Manager
Reynolds Electrical & Engineering Co.
Mail Stop 555
P.O. Box 98521
Las Vegas, NV 89193-8521

1 R. F. Pritchett
Technical Project Officer for YMP
Reynolds Electrical & Engineering Co.
MS 408
P.O. Box 98521
Las Vegas, NV 89193-8521

1 B. W. Colston
President/General Manager
Las Vegas Branch
Raytheon Services Nevada
MS 416
P.O. Box 95487
Las Vegas, NV 89193-5487

1 R. L. Bullock
Technical Project Officer for YMP
Raytheon Services Nevada
Suite P250, MS 403
101 Convention Center Dr.
Las Vegas, NV 89109

1 Paul Eslinger, Manager
PASS Program
Pacific Northwest Laboratories
P.O. Box 999
Richland, WA 99352

1 A. T. Tamura
Science and Technology Division
Office of Scientific and Technical Information
U.S. Department of Energy
P.O. Box 62
Oak Ridge, TN 37831

1 Carlos G. Bell, Jr.
Professor of Civil Engineering
Civil and Mechanical Engineering Department
University of Nevada, Las Vegas
4505 South Maryland Parkway
Las Vegas, NV 89154

1 P. J. Weeden, Acting Director
Nuclear Radiation Assessment Division
U.S. Environmental Protection Agency
Environmental Monitoring Systems Laboratory
P.O. Box 93478
Las Vegas, NV 89193-3478

1 ONWI Library
Battelle Columbus Laboratory
Office of Nuclear Waste Isolation
505 King Avenue
Columbus, OH 43201

1 T. Hay, Executive Assistant
Office of the Governor
State of Nevada
Capitol Complex
Carson City, NV 89710

3 R. R. Loux, Jr.
Executive Director
Nuclear Waste Project Office
State of Nevada
Evergreen Center, Suite 252
1802 North Carson Street
Carson City, NV 89710

1 C. H. Johnson
Technical Program Manager
Nuclear Waste Project Office
State of Nevada
Evergreen Center, Suite 252
1802 North Carson Street
Carson City, NV 89710

1 John Fordham
Water Resources Center
Desert Research Institute
P.O. Box 60220
Reno, NV 89506

1 David Rhode
Desert Research Institute
P. O. Box 60220
Reno, NV 89506

1 Eric Anderson
Mountain West Research-Southwest Inc.
2901 N. Central Ave. #1000
Phoenix, AZ 85012-2730

1 Department of Comprehensive Planning
Clark County
225 Bridger Avenue, 7th Floor
Las Vegas, NV 89155

1 Planning Department
Nye County
P.O. Box 153
Tonopah, NV 89049

1 Lincoln County Commission
Lincoln County
P.O. Box 90
Pioche, NV 89043

5 Judy Foremaster
City of Caliente
P.O. Box 158
Caliente, NV 89008

1 Economic Development Department
City of Las Vegas
400 East Stewart Avenue
Las Vegas, NV 89101

1 Community Planning & Development
City of North Las Vegas
P.O. Box 4086
North Las Vegas, NV 89030

1 Director of Community Planning
City of Boulder City
P.O. Box 61350
Boulder City, NV 89006

1 Commission of the European Communities
200 Rue de la Loi
B-1049 Brussels
BELGIUM

2 M. J. Dorsey, Librarian
YMP Research and Study Center
Reynolds Electrical & Engineering Co., Inc.
MS 407
P.O. Box 98521
Las Vegas, NV 89193-8521

1 Amy Anderson
Argonne National Laboratory
Building 362
9700 So. Cass Ave.
Argonne, IL 60439

1 Steve Bradhurst
P.O. Box 1510
Reno, NV 89505

1 Vernon Poe
P.O. Box 1026
Hawthorne, NV 89415

1 Jason Pitts
Lincoln County Courthouse
Pioche, NV 89043

1 Michael L. Baughman
35 Clark Road
Fiskdale, MA 01518

1 Glenn Van Roekel
Director of Community Development
City of Caliente
P.O. Box 158
Caliente, NV 89008

1 Ray Williams, Jr.
P.O. Box 10
Austin, NV 89310

1 Leonard J. Fiorenzi
P.O. Box 257
Eureka, NV 89316

1 Juanita Hayes
P.O. Box 490
Goldfield, NV 89013

1 Bjorn Selinder
190 W. First St.
Fallon, NV 89406

1 Charles Thistlethwaite, AICP
Associate Planner
Planning Department
Drawer L
Independence, CA 93526

1 Les Bradshaw
Nye County District Attorney
P.O. Box 593
Tonopah, NV 89049

1	6300	D. E. Miller
1	6302	T. E. Blejwas
1	6304	J. T. Holmes
1	6312	F. W. Bingham
1	6313	L. S. Costin
2	6318	R. J. Macer for 100/12411/SAND91-0558/NQ
1	6319	R. R. Richards
1	1600	P. J. Eicker
1	1611	P. A. Molley
1	1621	D. R. Strip
1	1661	R. W. Harrigan
1	1671	A. T. Jones
10	1671	W. D. Drotning
1	6115	P. J. Hommert, Acting
20	6341	WMT Library
1	6410	D. A. Dahlgren
5	7141	Technical Library
1	7151	Technical Publications
10	7613-2	Document Processing for DOE/OSTI
1	8523-2	Central Technical Files

SAND91-0558

The number in the lower right-hand corner is an accession number used for Office of Civilian Radioactive Waste Management purposes only. It should not be used when ordering this publication.

NNA.920806.0001

Org.	Bldg.	Name	Rec'd by	Org.	Bldg.	Name	Rec'd by

Sandia National Laboratories